

## **SUPPLEMENTAL DATA**

### **The energetic consequences of loop 9 gating motions in acetylcholine receptor-channels**

Archana Jha, Shaweta Gupta, Shoshanna N. Zucker and Anthony Auerbach  
Department of Physiology and Biophysics

Fig 1S

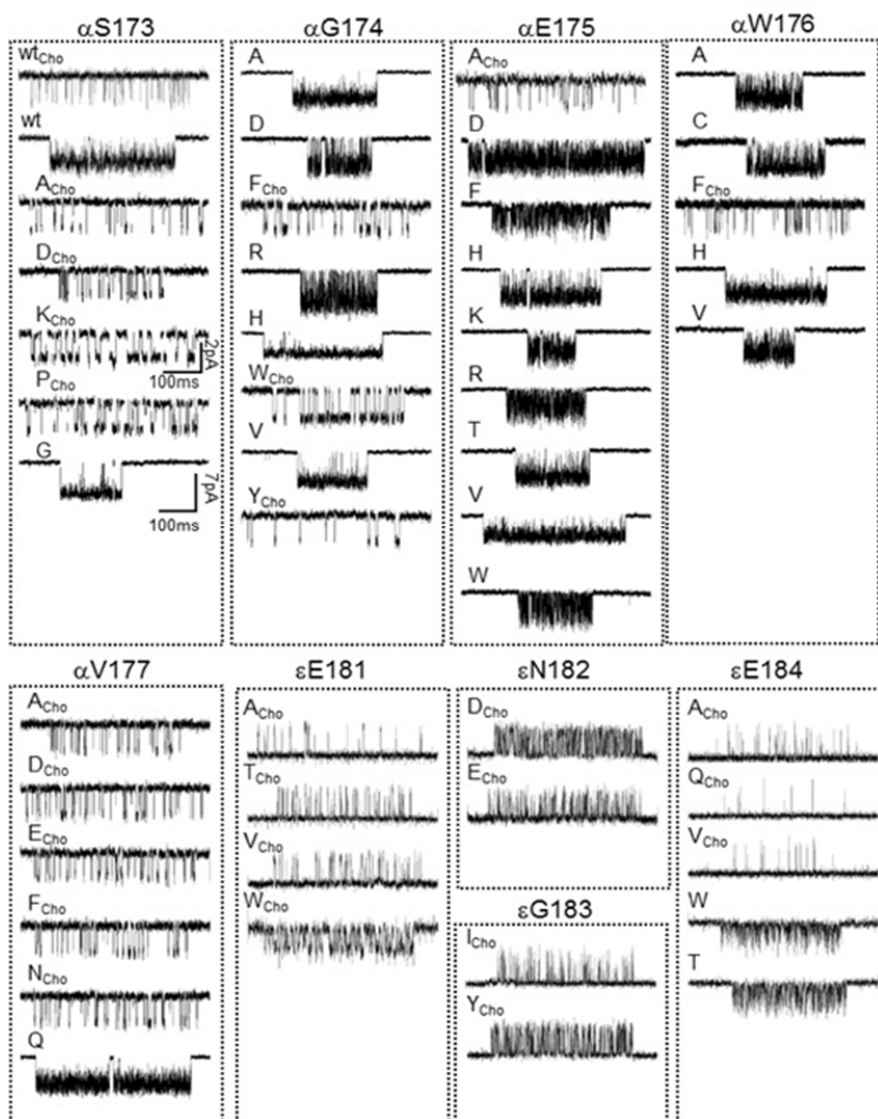


Fig. 1S. Example currents from mutant loop 9 residues. Currents were from AChRs activated by 500  $\mu$ M ACh unless noted by the subscript Cho (20 mM choline).

Fig 2S

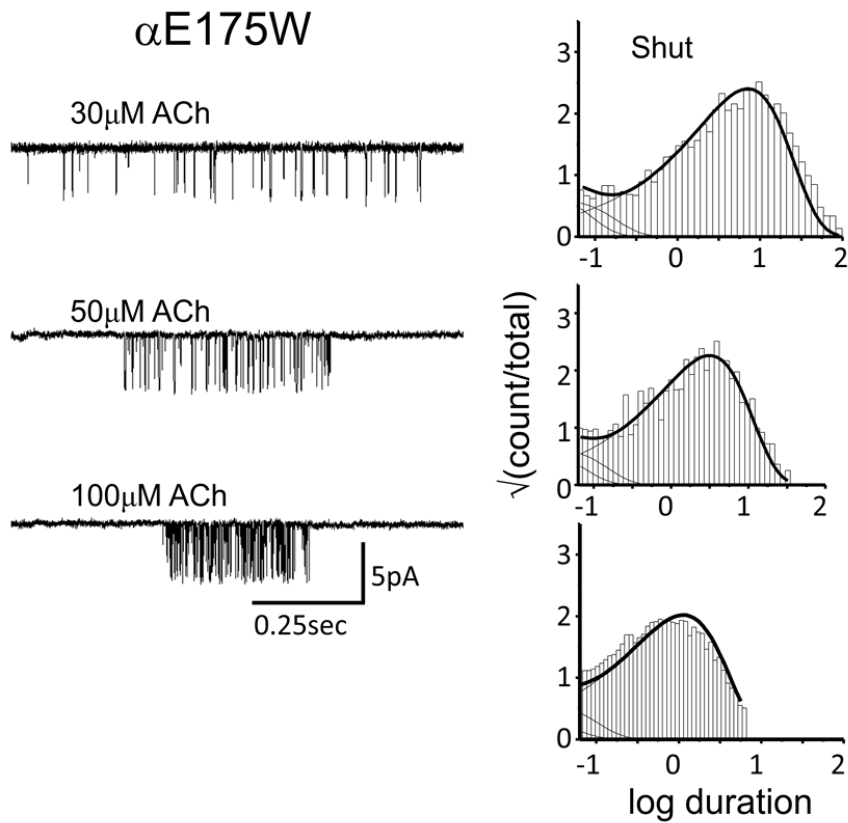


Fig. 2S. Estimating  $K_d$  for the  $\alpha L9$  mutant  $\alpha E175W$ . Left, current clusters elicited by different ACh concentrations. Right, corresponding shut-interval duration histograms. Solid lines were calculated from a global fit of the interval durations using a kinetic scheme with two equivalent binding sites (see Methods). The association and dissociation rate constant are:  $k_+ = 143 \pm 8 \mu M^{-1} s^{-1}$  and  $k_- = 17,433 \pm 1004 s^{-1}$  (mean  $\pm$  s.d.;  $K_d = 123 \mu M$ ). The values for wt AChRs activated by ACh are:  $k_+ = 167 \pm 8 \mu M^{-1} s^{-1}$  and  $k_- = 24,745 \pm 1004 s^{-1}$  ( $K_d = 148 \mu M$ ) (Chakrapani *et al.*, 2004)

Fig 3S

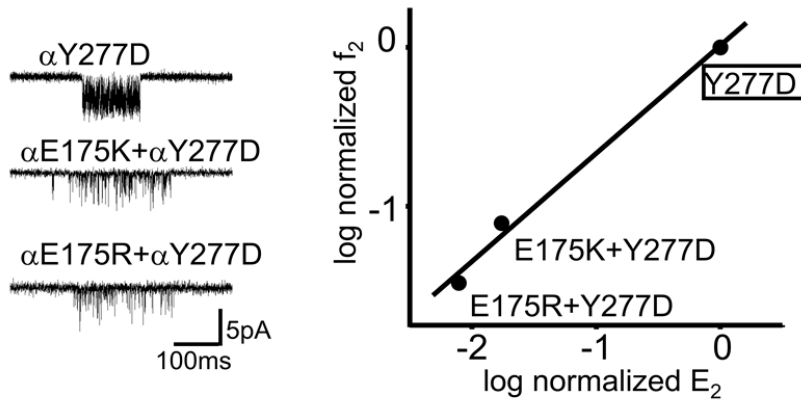


Fig. 3S. Kinetic analysis of  $\alpha Y277D$  (in  $\alpha M3$ ; see Fig. 1B), on different  $\alpha E175$  backgrounds. Left, example current clusters. Right, R-E plot. The  $\Phi$ -value of  $\alpha Y277$  (Cadugan & Auerbach, 2007) was not influenced by two  $\alpha E175$  side chains.

Fig 4S

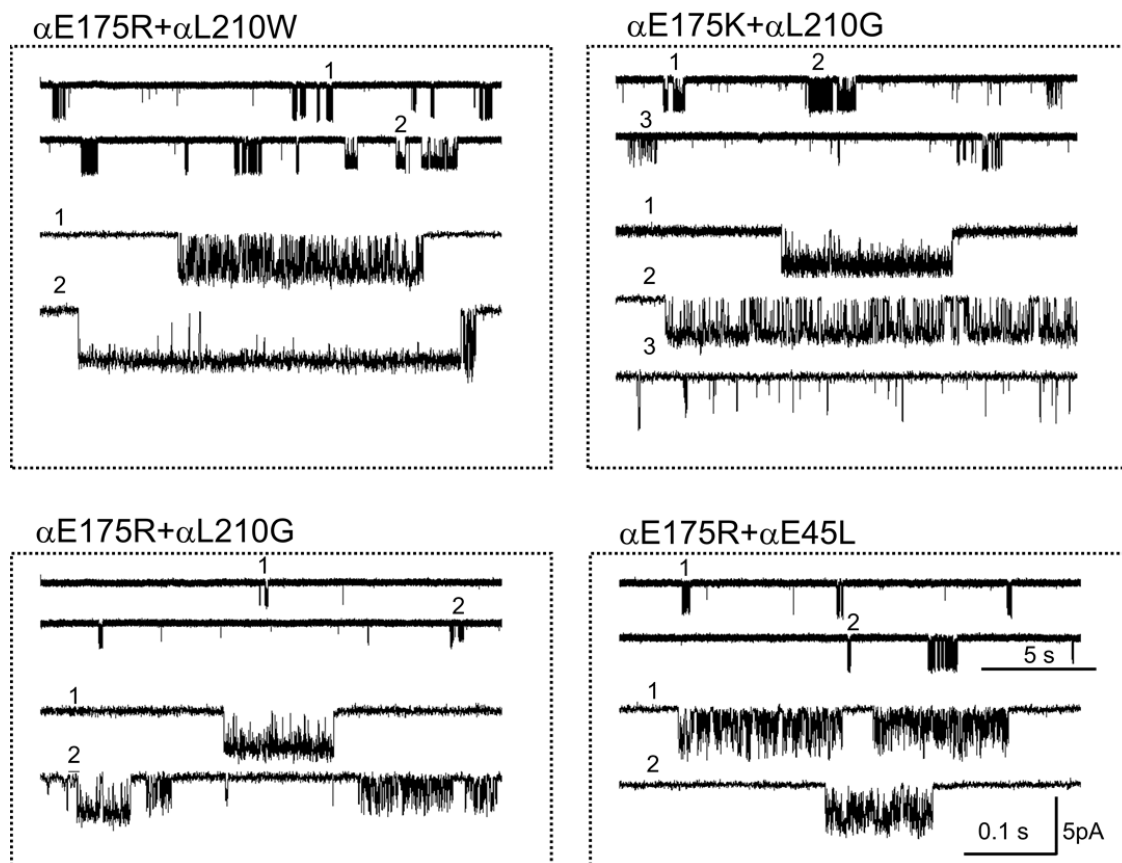


Fig. 4S. Example currents from multiply-mutated AChRs (E-T interface). The clusters for these mutant combinations showed heterogeneous kinetic properties.

Fig 5S

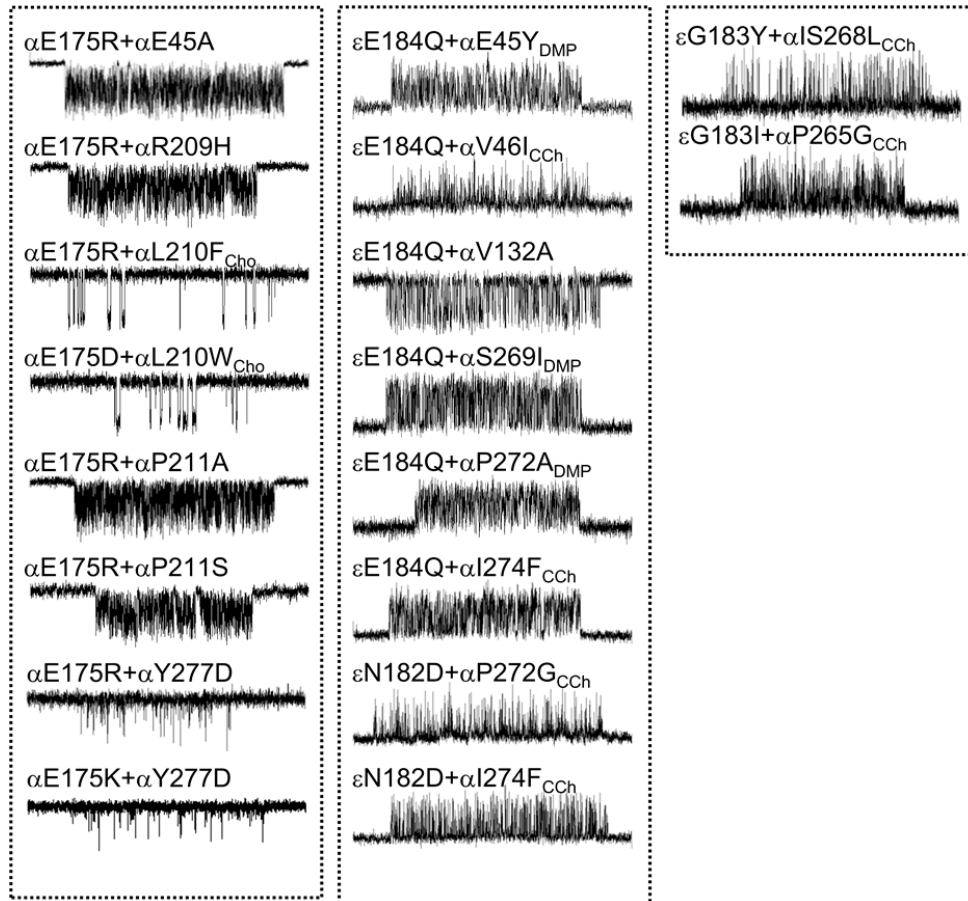


Fig. 5S. Example currents from multiply-mutated AChRs (E-T and P-C interfaces). The clusters for these mutant combinations did not show heterogeneous kinetic properties. Currents were from AChRs activated by 500  $\mu$ M ACh unless noted by the subscript Cho (20 mM choline), CCh (100 mM carbamylcholine) and DMP (100 mM dimethyl pyrrolidinium).

**Table 1S : Rate and equilibrium constants**

<b>Position</b>	<b>f<sub>2</sub><sup>obs</sup> (s<sup>-1</sup>)</b>	<b>b<sub>2</sub><sup>obs</sup> (s<sup>-1</sup>)</b>	<b>f<sub>2</sub><sup>corr</sup> (s<sup>-1</sup>)</b>	<b>b<sub>2</sub><sup>corr</sup> (s<sup>-1</sup>)</b>	<b>b<sub>2</sub><sup>*</sup> (s<sup>-1</sup>)</b>	<b>i<sub>0</sub> (pA)</b>	<b>i<sub>B</sub> (pA)</b>	<b>E<sub>2</sub><sup>corr</sup></b>	<b>Agonist</b>	<b>Fold-change in E<sub>2</sub></b>	<b>n</b>
wt <sub>Cho</sub> <sup>a</sup>	120	834		2583	2100	7	2	0.046	Cho	1.00	
wt <sub>Ach</sub> <sup>b</sup>	48000	-		1700	1000	7	5	28.2	ACh	1.00	
αS173A	82(4)	374(20)		1428	1012	6.3	1.65	0.057	Cho	1.24	3
αS173D	228(0.4)	549(50)		1983	1879	6.5	1.8	0.12	Cho	2.49	2
αS173G	28939(1302)	838(100)		1220	1127	6.7	4.6	23.7	ACh	0.84	3
αS173K	74(9)	115(7)		399	440	6.6	1.9	0.19	Cho	4.10	2
αS173P	104(1)	251(16)		879	1097	6.3	1.8	0.12	Cho	2.60	3
αG174A	25094(2770)	1433(274)		1874	1674	6.8	5.2	13.4	ACh	0.47	3
αG174D	1867(228)	885(111)		1062	931	5.2	4.3	1.75	ACh	0.062	4
αG174F	101(17)	271(13)		1070	608	7.5	1.9	0.09	Cho	1.95	3
αG174H	26578(1440)	975(264)		1099	794	5.3	4.7	24.18	ACh	0.85	3
αG174R	10420(1039)	1282(51)		1910	1882	7.3	4.9	5.45	ACh	0.19	3
αG174W	99(26)	195(48)		871	641	6.7	1.5	0.11	Cho	2.47	3
αG174V	24495(1296)	985(152)		1174	1115	6.2	5.2	20.86	ACh	0.74	3
αG174Y	32(1.8)	398(40)		2044	1527	7.5	1.46	0.016	Cho	0.35	3
αE175A	75(16)	674(65)		2152	2087	5.1	1.6	0.03	Cho	0.75	3
αE175C <sup>c</sup>	-	-		-	-	-	-	-	ACh	-	3
αE175D	15331(618)	3746(736)		4263	3240	7	6.15	3.59	ACh	0.13	3
αE175F <sup>c</sup>	-	-		-	-	-	-	-	ACh	-	3
αE175H	13716(1015)	1399(184)		2072	1965	7.1	4.8	6.6	ACh	0.23	3
αE175K	10014(1219)	3215(889)		5296	4723	6.9	4.2	1.89	ACh	0.07	2
αE175Q <sup>c</sup>	-	-		-	-	-	-	-	ACh	-	3
αE175R	7676 (948)	6405(391)		7419	7706	7	6.04	1.03	ACh	0.036	3
αE175R <sub>Hyb</sub>	16982	2815		4582		7	4.3	3.7	ACh	0.13	3
αE175T	16437 (677)	713(84)		1283	776	7.2	4.0	12.8	ACh	0.45	3
αE175V	19581	2365		2819	1124	6.2	5.2	6.9	ACh	0.25	1
αE175W	4750(870)	4608(259)		5642	5781	6	4.9	0.84	ACh	0.029	3
αE175Y <sup>c</sup>	-	-		-	-	-	-	-	ACh	-	3
αW176H	25366(743)	1562(134)		1952	2073	6	4.8	12.9	ACh	0.46	3
αW176F	157(25)	1109(58)		3716	4052	6.7	2	0.04	Cho	0.92	2
αW176C	12151(785)	1586(247)		2241	2606	6.5	4.6	5.4	ACh	0.19	3
αW176A	8573(869)	1728(111)		2298	2480	6.5	4.9	3.73	ACh	0.13	3

$\alpha$ W176V	13371(701)	2254(236)		3255	1722	6.0	4.1	5.05	ACh	0.15	2
$\alpha$ V177A	135(9)	832(223)		3432	3262	6.6	1.6	0.04	Cho	0.87	4
$\alpha$ V177D	178(1.5)	942(102)		3706	2565	6.3	1.6	0.048	Cho	1.0	2
$\alpha$ V177E	95(21)	866(174)		3983	1516	6.9	1.5	0.024	Cho	0.52	3
$\alpha$ V177F	112	779		2548	2119	7	2.1	0.044	Cho	0.95	1
$\alpha$ V177N	112(19)	809(24)		3438	2859	7	1.7	0.03	Cho	0.71	3
$\alpha$ V177Q	34468(2806)	702(73)		974	1195	6.9	5	35.38	ACh	1.25	3
$\epsilon$ E181A <sup>d</sup>	15	1312	11.5	820				0.01	Cho	0.3	1
$\epsilon$ E181T <sup>d</sup>	180(55)	2073(36)	138	1295				0.11	Cho	2.2	2
$\epsilon$ E181V <sup>d</sup>	289(120)	1216(66)	222	760				0.29	Cho	6.1	2
$\epsilon$ E181W <sup>d</sup>	1021(9)	1352	785	845				0.93	Cho	19.4	2
$\epsilon$ N182D <sup>d</sup>	1898	1730	1460	912				1.60	Cho	33.3	3
$\epsilon$ N182E <sup>d</sup>	717	3233(14)	551	2020				0.27	Cho	5.7	3
$\epsilon$ G183I <sup>d</sup>	494(30)	4249(1035)	380	2655				0.14	Cho	3.0	3
$\epsilon$ G183Y <sup>d</sup>	1121	3264	862	2040				0.42	Cho	8.8	1
$\epsilon$ E184W	1040(158)	9386(285)	800	5866				0.11	ACh	0.004	2
$\epsilon$ E184T	3431	9869	2639	6168				0.34	ACh	0.012	1
$\epsilon$ E184Q <sup>d</sup>	22	4677	17	2923				0.01	Cho	0.12	1
$\epsilon$ E184A <sup>d</sup>	47(11)	3670(371)	36	2294				0.02	Cho	0.3	3
$\epsilon$ E184V <sup>d</sup>	16	4496	12	2810				0.004	Cho	0.09	1

$f_2^{\text{obs}}$  is the observed forward, channel-opening rate constant;  $b_2^{\text{obs}}$  is the observed backward, channel-closing rate constant;  $f_2^{\text{corr}}$  is the opening rate constant corrected for the background mutation;  $b_2^{\text{corr}}$  is the closing rate constant corrected for channel block (see Methods);  $b_2^*$  is the diliganded closing rate constant measured at a low agonist concentration;  $i_0$  is the single-channel current amplitude at a low agonist concentration (no block);  $i_B$  is the observed channel current amplitude at a high agonist concentration (with block);  $E_2^{\text{corr}}$  is the corrected diliganded gating equilibrium constant ( $=f_2^{\text{corr}}/b_2^{\text{corr}}$ ), which is for -70 mV, 23 °C; the agonist was either acetylcholine (ACh) or choline (Cho);  $n$ , the number of patches. Values are mean ( $\pm$ SE). a, from (Chakrapani *et al.*, 2003) and b, from (Mitra *et al.*, 2005). c, rate constants not estimated because of heterogenous cluster kinetics. d, corrected for the background condition (+70 mV,  $\alpha$ V283W) (Cadugan & Auerbach, 2007).

**TABLE 2S: Coupling energies**

Construct	$f_2^{\text{obs}}$ (s <sup>-1</sup> )	$b_2^{\text{obs}}$ (s <sup>-1</sup> )	$f_2^{\text{corr}}$ (s <sup>-1</sup> )*	$b_2^{\text{corr}}$ (s <sup>-1</sup> )*	$E_2^{\text{corr}}$	E <sub>2</sub> fold change		Agonist	$\Delta\Delta G$ (kcal/mol)	n
						observed	predicted			
$\alpha$ E175R+ $\alpha$ E45A	8786(414)	7789(1517)		12981	0.67	0.023	.0036	ACh	-1.09	2
$\alpha$ E175R+ $\alpha$ E45L <sup>a</sup>	-	-		-	-	-	-	ACh	-	3
$\alpha$ E175R+ $\alpha$ R209H	8819(952)	8455(15)		11778	0.75	0.026	0.029	ACh	+0.053	2
$\alpha$ E175K+ $\alpha$ L210G <sup>a</sup>	-	-		-	-	-	-	ACh	-	4
$\alpha$ E175R+ $\alpha$ L210G <sup>a</sup>	-	-		-	-	-	-	ACh	-	3
$\alpha$ E175R+ $\alpha$ L210F	41(4)	287(71)		913	.045	0.97	0.22	Cho	-0.87	2
$\alpha$ E175D+ $\alpha$ L210W	77(9)	382(19)		1216	0.063	1.37	1.39	Cho	-	2
$\alpha$ E175R+ $\alpha$ L210W <sup>a</sup>	-	-		-	-	-	-		-	
$\alpha$ E175R+ $\alpha$ P211A	3149(190)	1684(145)		3185	0.98	0.035	.012	ACh	-0.65	3
$\alpha$ E175R+ $\alpha$ P211S	4236	1552		3104	1.36	0.05	.05	ACh	-	1
$\beta$ K46E	13982(474)	2856(645)		3702	3.8	0.13		ACh		
$\alpha$ E175R+ $\beta$ K46E	883(207)	19795(2892)		32992	.027	0.00095	.0048	ACh	+0.96	3
$\alpha$ E175R+ $\alpha$ Y277D	364(83)	17381(803)		30417	.012	0.00042	.0018	ACh	+0.90	3
$\alpha$ E175K+ $\alpha$ Y277D	869(63)	19287(856)		32929	0.026	0.00092	.0035	ACh	+0.81	3
$\epsilon$ E184Q+ $\alpha$ E45Y <sup>b</sup>	1927(264)	2588(381)	2698	863	3.13	8.24	7.58	DMP	-0.05	2
$\epsilon$ E184Q+ $\alpha$ V46I <sup>b</sup>	1799 (182)	13160(641)	2519	4387	0.57	0.11	0.06	CCh	-0.36	2
$\epsilon$ E184Q+ $\alpha$ V132A	709(89)	1356(186)		2034	0.35	0.012	0.016	ACh	+0.47	2
$\epsilon$ E184Q+ $\alpha$ S269I <sup>b</sup>	1839(390)	1692(221)	2575	564	4.6	0.86	2.6	DMP	+0.65	2
$\epsilon$ E184Q+ $\alpha$ P272A <sup>b</sup>	4861(412)	1381(83)	6805	460	14.8	2.8	5.3	DMP	+0.38	2
$\epsilon$ E184Q+ $\alpha$ I274F <sup>c</sup>	4075 (216)	1683(131)	1132	2475	0.46	0.086	0.0062	CCh	-1.56	2
$\epsilon$ N182D+ $\alpha$ P272G <sup>b</sup>	1095	12376	1521	4175	0.36	0.068	0.125	CCh	+0.36	1
$\epsilon$ N182D+ $\alpha$ I274F <sup>b</sup>	1543(42)	6065(826)	2143	2046	1.05	0.20	0.25	CCh	+0.13	2
$\epsilon$ G183I+ $\alpha$ P265G <sup>b</sup>	3082(286)	11689(647)	4281	3943	1.08	0.20	0.07	CCh	-1.7	2
$\epsilon$ G183Y+ $\alpha$ S268L <sup>b</sup>	842(16)	5811(734)	1169	1960	0.6	0.11	0.18	CCh	+0.3	2

See Table 1S legend.  $E_2$  fold change: observed,  $E_2^{\text{mut}}/E_2^{\text{wt}}$ ; predicted, product of  $E_2^{\text{corr}}$  for each mutant pair;  $\Delta\Delta G$ , coupling energy is calculated as described in the Methods. Agonists were acetylcholine (ACh), choline (Cho), carbamylcholine (CCh) or dimethyl pyrrolidinium (DMP) (Jadey *et al.*, 2011). a, not estimated because of heterogeneous kinetics; b, expressed on the  $\beta$ T464I background (Mitra *et al.*, 2005); c, expressed on the  $\beta$ (L269D+T464F) background (Jadey,S.V., Purohit,P. and Auerbach,A. 2009.Biophysical Society.Abstr.862-Pos.)

## REFERENCES

- Cadugan DJ & Auerbach A. (2007). Conformational dynamics of the alphaM3 transmembrane helix during acetylcholine receptor channel gating. *Biophys J* **93**, 859-865.
- Chakrapani S, Bailey TD & Auerbach A. (2003). The role of loop 5 in acetylcholine receptor channel gating. *J Gen Physiol* **122**, 521-539.
- Chakrapani S, Bailey TD & Auerbach A. (2004). Gating dynamics of the acetylcholine receptor extracellular domain. *J Gen Physiol* **123**, 341-356.
- Jadey SV, Purohit P, Bruhova I, Gregg TM & Auerbach A. (2011). Design and control of acetylcholine receptor conformational change. *Proc Natl Acad Sci U S A* **108**, 4328-4333.
- Mitra A, Cymes GD & Auerbach A. (2005). Dynamics of the acetylcholine receptor pore at the gating transition state. *Proc Natl Acad Sci U S A* **102**, 15069-15074.